Supplementary Information

TREM1 signaling amplifies neutrophil-mediated inflammation in inflammatory bowel disease

Warrison Andrade[1], Hao Xu[2], Yutian Peng[3], Zhiyuan Yao[4], Jack Bevers[5], Rhyan Puno[6], Yongchang Shi[7], Victoria Pham[8], Meena Choi[8], Yonglian Sun[5], Alexis Scherl[9], Ruoyu Zhang[4], Alexandra Paun[10], Tao Sun[11], Yuxin Liang[8], Nandhini Ramamoorthi[12], Jianyong Wang[7], Dhaya Seshasayee[5], Gerald Nakamura[5], Man-Wah Tan[3], Hua Zhang[2], Mary Keir[1], Jason Hackney[4], Saiyu Hang[1]*

1 Immunology Discovery, Genentech, South San Francisco, CA 94080, USA.

2 Translational Immunology, Genentech, South San Francisco, CA 94080, USA.

3 Infectious Diseases and Host-Microbe Interactions, Genentech, South San Francisco, CA 94080, USA.

4 OMNI Bioinformatics, Genentech, South San Francisco, CA 94080, USA.

5 Antibody Engineering, Genentech, South San Francisco, CA 94080, USA.

6 Structural Biology, Genentech, South San Francisco, CA 94080, USA.

7 Biochemical and Cellular Pharmacology, Genentech, South San Francisco, CA 94080, USA.

8 Proteomic and Genomic Technologies, Genentech, South San Francisco, CA 94080, USA.

9 Research Pathology, Genentech, South San Francisco, CA 94080, USA.

10 Computational Biology, Roche, Basel, Switzerland.

11 Molecular Biology, Genentech, South San Francisco, CA 94080, USA.

12 Pharma Biosample Services, Genentech, South San Francisco, CA 94080, USA.

* Correspondence: hang.saiyu@gene.com (S.H.)

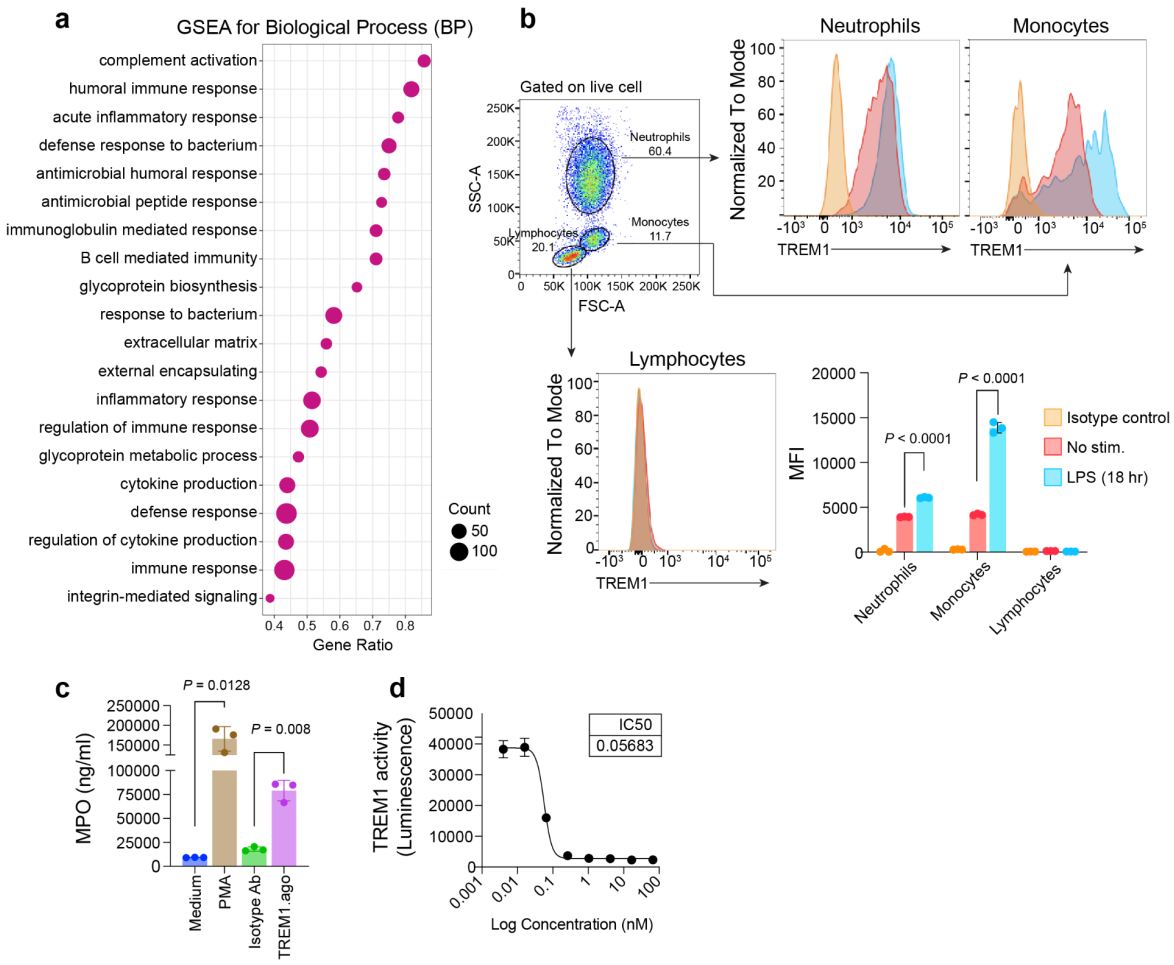

Supplementary Fig. 1 TREM1 regulates neutrophil activities

a, Gene set enrichment analysis (GSEA) of the neutrophil secretome proteomics, showing the top 20 pathways enriched in PMA-stimulated vs DMSO-treated neutrophils (FDR < 0.01). **b**, Surface TREM1 expression on blood leukocytes from healthy donors after 18 h LPS stimulation, quantified by flow cytometry as geometric mean fluorescence intensity (MFI). Each point represents one donor (n = 3); data are mean ± SD. Two-sided unpaired t-tests were used. **c**, MPO release from neutrophils stimulated overnight with PMA, plate-bound TREM1.ago or isotype control. Each point represents one donor (n = 3); data are mean ± SD. Two-sided unpaired t-tests with Welch's correction were used. **d**, Dose-response of the anti-TREM1 blocking antibody in an NFAT-NanoLuc reporter line expressing human TREM1 and DAP12, stimulated with PGN/PGLYRP1; luminescence reflects TREM1 pathway activity.

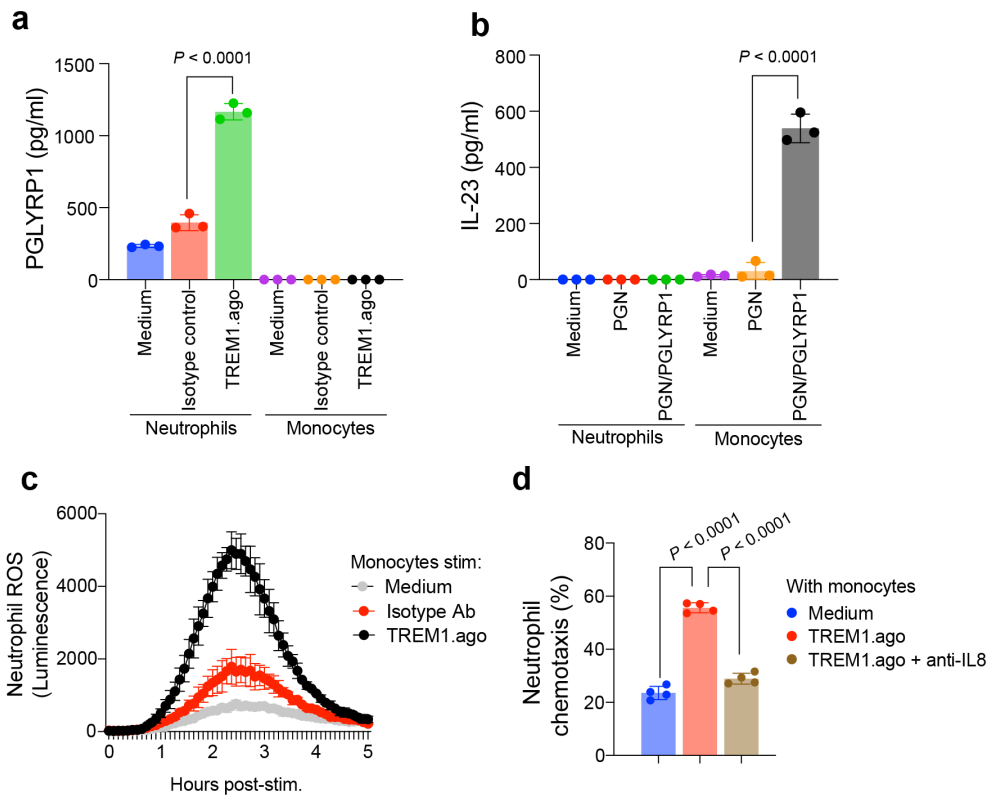

Supplementary Fig. 2 TREM1 activation on monocytes induces neutrophil ROS production and chemotaxis.

a-b, Neutrophils or monocytes purified from healthy donors (n = 3 donors per cell type) were stimulated with plate-bound TREM1.ago or isotype (a), and PGLYRP1 levels in supernatants were measured by ELISA (PGLYRP1 primarily from neutrophils), or with PGN alone or PGN/PGLYRP1 (b), and IL-23 secretion was measured by ELISA (restricted to monocytes). Each point represents one donor; data are mean ± SD. Two-sided unpaired t-tests were used.

c-d, As schematized in Fig. 2d, monocytes were stimulated with plate-bound TREM1.ago or isotype, and supernatants were collected and used to treat neutrophils. (c) ROS production over time in neutrophils exposed to monocyte supernatants (n = 3 donors); curves show mean ± SD. (d) Neutrophil chemotaxis toward monocyte supernatants in the presence or absence of anti-IL-8 (n = 4 donors). Each point represents neutrophils from one donor; data are mean ± SD. Two-sided unpaired t-tests were used for chemotaxis comparisons.

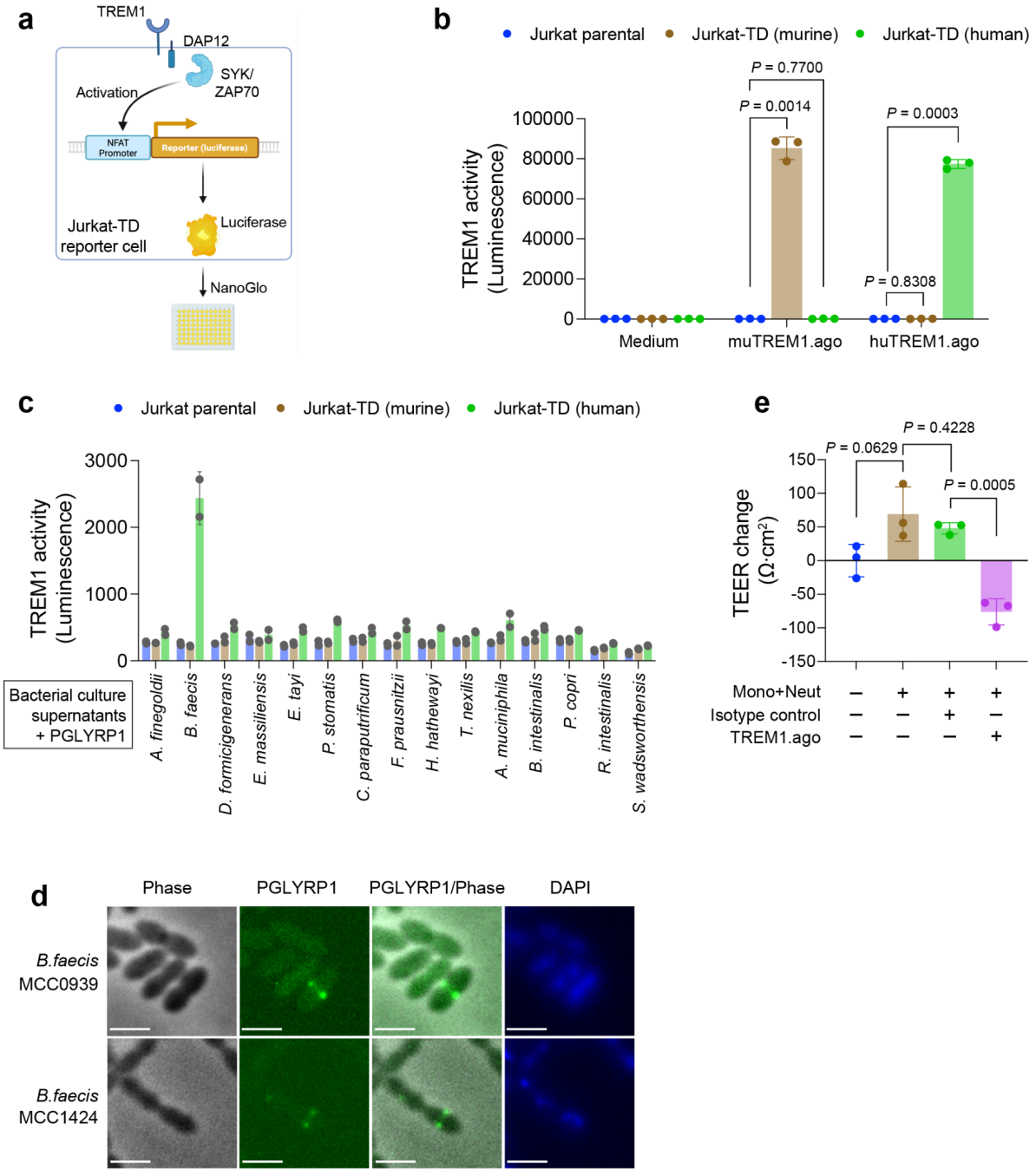

Supplementary Fig. 3 Activities of gut commensal bacteria on human vs. murine TREM1

a, Schematic of the Jurkat-TD NFAT-NanoLuc TREM1 reporter system. Created in BioRender. Hang, S. (2026) https://BioRender.com/38t8tbv. Cells express either human TREM1/DAP12 (Jurkat-TD, human) or murine TREM1/DAP12 (Jurkat-TD, murine); TREM1 activation triggers

NFAT-driven luciferase expression. **b**, Human vs murine TREM1 reporter activity in Jurkat-TD cells stimulated with plate-bound human or murine TREM1 agonist antibodies (n = 3 independent experiments; mean ± SD). Two-sided unpaired t-tests with Welch's correction were used. **c**, Screen of culture supernatants from 15 gut commensal species isolated from IBD patients, tested for activation of human TREM1 in Jurkat-TD cells in the presence of recombinant PGLYRP1 (n = 2 independent experiments; mean ± SD). 15 species include: *Alistipes finegoldii* (*A. finegodii*), *Blautia faecis (B. faecis*), *Dorea formicigenerans* (*D. fomicigenerans*), *Eisenbergiella massiliensis* (*E. massiliensis*), *Eisenbergiella tayi* (*E. tayi*), *Peptostreptococcus stomatis* (*P. stomatis*), *Clostridium paraputrificum* (*C. paraputrificum*), *Faecalibacterium prausnitzii* (*F. prausnitzii*), *Hungatella hathewayi* (*H. hathewayi*), *Tyzzerella nexilis* (*T. nexilis*), *Akkermansia muciniphila* (*A. muciniphila*), *Bacteroides intestinalis* (*B. intestinalis*), *Prevotella copri* (*P. copri*), *Roseburia intestinalis* (R. intestinalis), *Sutterella wadsworthensis* (*S. wadsworthensis*). **d**, Immunofluorescence staining of live *B. faecis* strains MCC0939 and MCC1424 incubated with recombinant human PGLYRP1. Bacteria were stained with anti-PGLYRP1 antibody (green) and DNA dye (blue). Control samples without PGLYRP1 or with an isotype antibody show minimal staining. Images are representative of n = 3 independent experiments. Scale bar, 2 μm. **e**, TEER assay assessing gut epithelial barrier integrity. Caco-2 monolayers were grown on transwells; monocytes and neutrophils from healthy donors (n = 3) were placed in the lower chamber and stimulated with plate-bound TREM1.ago or isotype control. Each point represents one donor; data are mean ± SD. Two-sided unpaired t-tests were used. The TEER assay setup is illustrated in Fig. 3h.

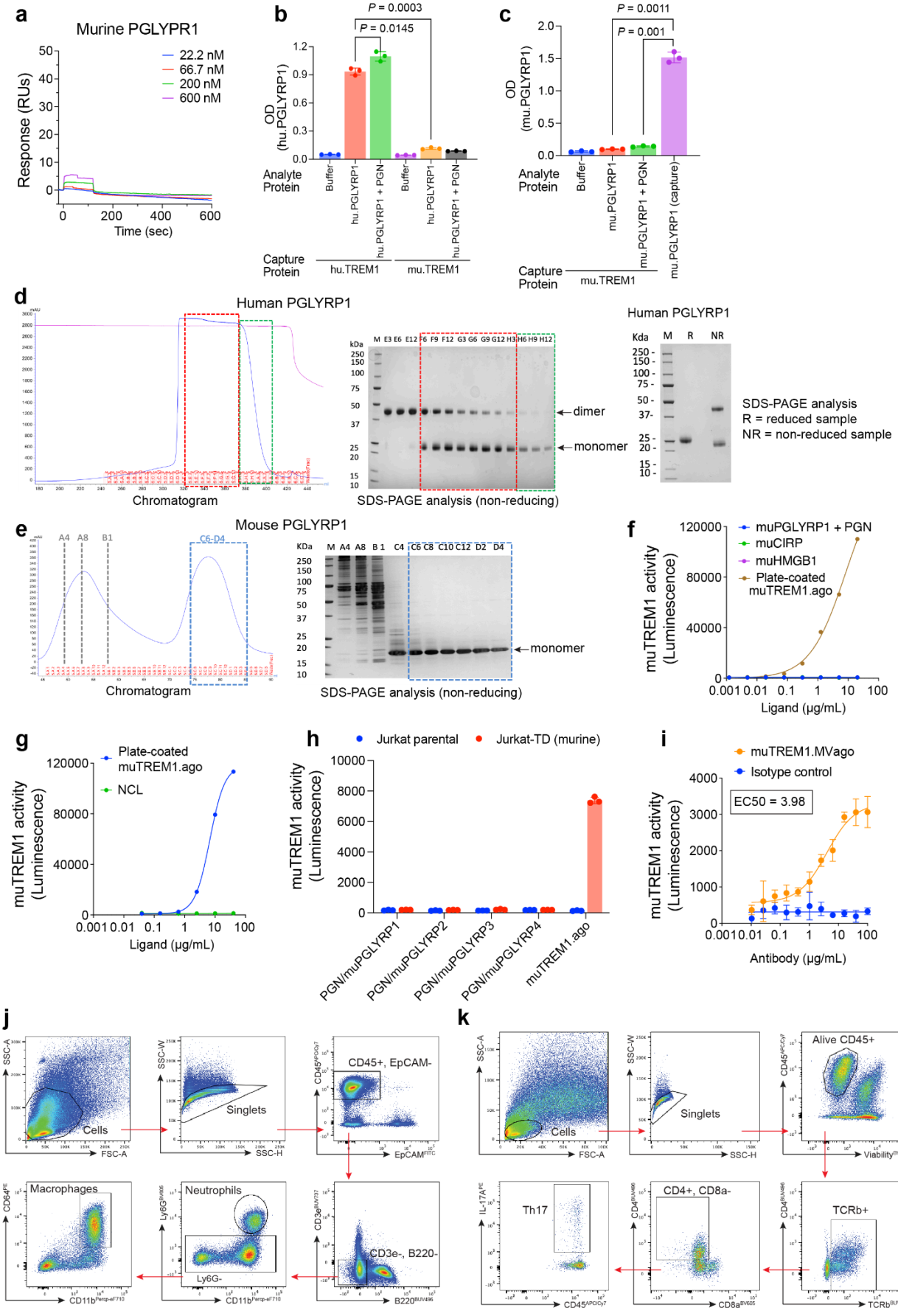
a
Murine PGLYPR1
22.2 nM
66.7 nM
200 nM
600 nM
Response (RUs)
Time (sec)
b
P = 0.0003
P = 0.0145
OD (hu.PGLYRP1)
Analyte Protein
Buffer
hu.PGLYRP1
hu.PGLYRP1 + PGN
Capture Protein
hu.TREM1
mu.TREM1
c
P = 0.0011
P = 0.001
OD (mu.PGLYRP1)
mu.PGLYRP1
mu.PGLYRP1 + PGN
mu.PGLYRP1 (capture)
d
Human PGLYRP1
Chromatogram
SDS-PAGE analysis (non-reducing)
dimer
monomer
Kda
M
R
NR
SDS-PAGE analysis
R = reduced sample
NR = non-reduced sample
e
Mouse PGLYRP1
A4
A8
B1
C6-D4
Chromatogram
SDS-PAGE analysis (non-reducing)
monomer
f
muPGLYRP1 + PGN
muCIRP
muHMGB1
Plate-coated muTREM1.ago
muTREM1 activity (Luminescence)
Ligand (µg/mL)
g
Plate-coated muTREM1.ago
NCL
muTREM1 activity (Luminescence)
Ligand (µg/mL)
h
Jurkat parental
Jurkat-TD (murine)
muTREM1 activity (Luminescence)
PGN/muPGLYRP1
PGN/muPGLYRP2
PGN/muPGLYRP3
PGN/muPGLYRP4
muTREM1.ago
i
muTREM1.MVago
Isotype control
EC50 = 3.98
muTREM1 activity (Luminescence)
Antibody (µg/mL)
j
Cells
Singlets
CD45+, EpCAM-
Macrophages
Neutrophils
Ly6G-
CD3e-, B220-
k
Cells
Singlets
Alive CD45+
Th17
CD4+, CD8a-
TCRb+

Supplementary Fig. 4 Murine TREM1 is not activated by PGLYRP1, CIRP or necrotic cell lysate

a, SPR analysis of binding between murine TREM1-Fc and murine PGLYRP1, showing lack of detectable interaction. **b-c**, Protein-protein interaction ELISA for PGLYRP1-TREM1 binding. (b) Human or mouse TREM1-Fc was coated as capture; human PGLYRP1 ± PGN was added as analyte, and binding was detected with anti-human PGLYRP1. Human PGLYRP1 binds human, but not mouse, TREM1. (c) Mouse TREM1-Fc was coated as capture; mouse PGLYRP1 ± PGN was added as analyte, and binding was detected with anti-mouse PGLYRP1. Mouse PGLYRP1 coated directly on the plate served as positive control. **d-e**, Biochemical properties of human and mouse PGLYRP1. Human (d) and mouse (e) PGLYRP1 constructs with N-terminal Flag tags were expressed in HEK293 cells, purified on anti-Flag resin and separated by SEC (Superdex S200 for human, S75 for mouse). Fractions were analyzed by SDS-PAGE under reducing and non-reducing conditions, revealing disulfide-linked dimerization of human but not mouse PGLYRP1. **f-g**, Dose-response activation of murine TREM1 in TREM1-TD (murine) reporter cells by candidate ligands (murine PGLYRP1, CIRP, HMGB1, necrotic cell lysate (NCL)) compared with plate-bound muTREM1.ago. **h**, Murine TREM1 activity upon stimulation with PGN (from *E. coli*) complexed with murine PGLYRP1, PGLYRP2, PGLYRP3 or PGLYRP4 (n = 3 independent experiments; mean ± SD); plate-bound muTREM1.ago served as a positive control. **i**, In-solution potency of the multivalent muTREM1 agonist, muTREM1.MVago, in murine TREM1-TD cells (n = 3 independent experiments; mean ± SD). **j-k**, Gating strategies for immune cell populations in the DSS colitis model. (j) Example gating of colon lamina propria cells to define neutrophils ($CD11b^+Ly6G^+Ly6C$^int) and macrophages ($CD11b^+Ly6G^-Ly6C^-CD64^+$); this corresponds to neutrophil/macrophage quantification in Fig. 4f,g,i,j. (k) Gating of $CD4^+$ T cells ($CD45^+CD4^+TCR\beta^+$) and intracellular IL-$17A^+$ Th17 cells; this corresponds to Th17 quantification in Fig. 4h,k.

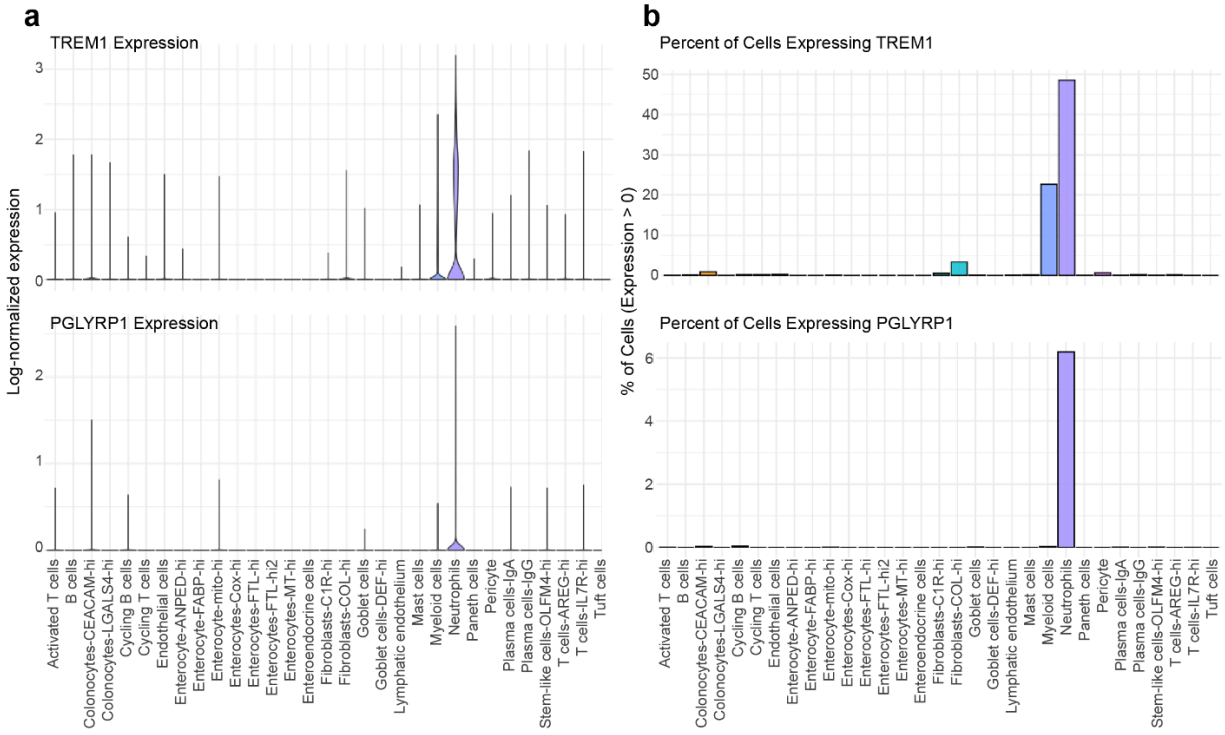
a
TREM1 Expression
PGLYRP1 Expression
Log-normalized expression
b
Percent of Cells Expressing TREM1
Percent of Cells Expressing PGLYRP1
% of Cells (Expression > 0)
Activated T cells
B cells
Colonocytes-CEACAM-hi
Colonocytes-LGALS4-hi
Cycling B cells
Cycling T cells
Endothelial cells
Enterocyte-ANPED-hi
Enterocyte-FABP-hi
Enterocyte-mito-hi
Enterocytes-Cox-hi
Enterocytes-FTL-hi
Enterocytes-FTL-hi2
Enterocytes-MT-hi
Enteroendocrine cells
Fibroblasts-C1R-hi
Fibroblasts-COL-hi
Goblet cells
Goblet cells-DEF-hi
Lymphatic endothelium
Mast cells
Myeloid cells
Neutrophils
Paneth cells
Pericyte
Plasma cells-IgA
Plasma cells-IgG
Stem-like cells-OLFM4-hi
T cells-AREG-hi
T cells-IL7R-hi
Tuft cells

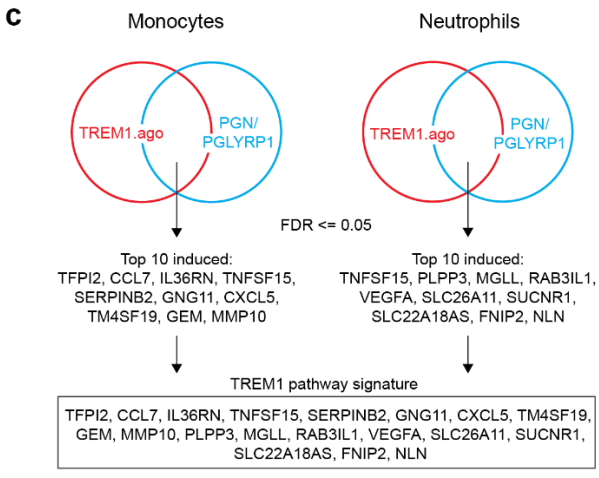
c
Monocytes
Neutrophils
TREM1.ago
PGN/
PGLYRP1
FDR <= 0.05
Top 10 induced:
TFPI2, CCL7, IL36RN, TNFSF15,
SERPINB2, GNG11, CXCL5,
TM4SF19, GEM, MMP10
Top 10 induced:
TNFSF15, PLPP3, MGLL, RAB3IL1,
VEGFA, SLC26A11, SUCNR1,
SLC22A18AS, FNIP2, NLN
TREM1 pathway signature
TFPI2, CCL7, IL36RN, TNFSF15, SERPINB2, GNG11, CXCL5, TM4SF19,
GEM, MMP10, PLPP3, MGLL, RAB3IL1, VEGFA, SLC26A11, SUCNR1,
SLC22A18AS, FNIP2, NLN

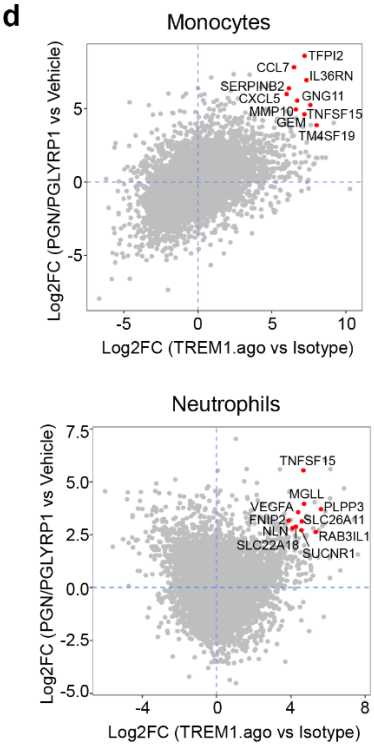
d
Monocytes
TFPI2
CCL7
IL36RN
SERPINB2
CXCL5
GNG11
MMP10
TNFSF15
GEM
TM4SF19
Log2FC (PGN/PGLYRP1 vs Vehicle)
Log2FC (TREM1.ago vs Isotype)
Neutrophils
TNFSF15
MGLL
VEGFA
PLPP3
FNIP2
SLC26A11
NLN
RAB3IL1
SLC22A18
SUCNR1
Log2FC (PGN/PGLYRP1 vs Vehicle)
Log2FC (TREM1.ago vs Isotype)

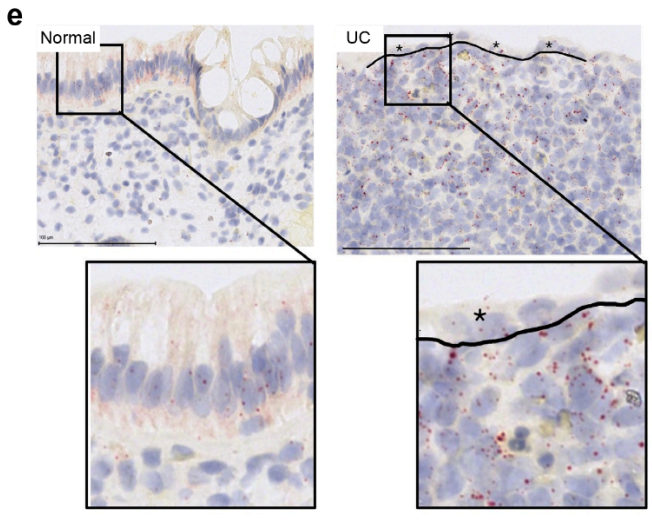
e
Normal
UC

Supplementary Fig. 5 TREM1 and PGLYRP1 expression in IBD biopsies and pathway signature construction

a-b, Single-cell RNA-seq analysis of Crohn's disease biopsies, showing cell-type specific expression of *TREM1* and *PGLYRP1* using a public dataset[1]. (a) Normalized expression per cell across annotated cell types. (b) Percentage of cells expressing each gene within each cell-type cluster. **c**, Schematic of the derivation of the TREM1 pathway gene signature from TREM1-activated human monocytes and neutrophils. **d**, Two-way plot highlighting the top 10 genes induced by both TREM1.ago and PGN/PGLYRP1 in monocytes and the top 10 in neutrophils (FDR ≤ 0.05). **e**, TREM1 in situ hybridization (RNAscope) in human colon biopsies. Left, normal colonic mucosa with low-level TREM1 transcripts (1-3 per cell) in surface epithelium and scattered lamina propria immune cells. Right, ulcerative colitis biopsy with severe active disease showing high TREM1 signal in granulation tissue underlying wound-associated epithelium (asterisks). Scale bar, 100 μm.

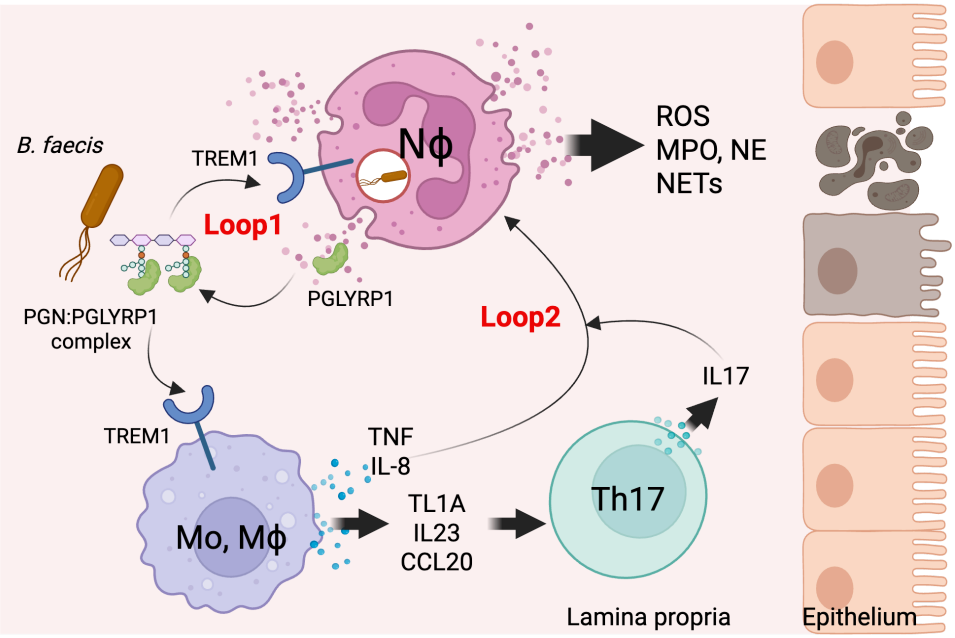

Supplementary Fig. 6 Model of the TREM1 pathogenic mechanism in IBD

Schematic model of TREM1-driven amplification loops in IBD. Loop 1: activation of existing neutrophils leads to degranulation and release of PGLYRP1, which binds bacterial peptidoglycan (PGN) to form a ligand complex that activates TREM1. TREM1 signaling enhances neutrophil effector functions, including ROS production, degranulation and NETosis, releasing additional PGLYRP1 and amplifying the loop. Loop 2: TREM1 activation in monocytes induces secretion of cytokines (TNF, TL1A, IL-23) and chemokines (IL-8, CCL20). IL-8 and TNF directly recruit and activate neutrophils, whereas CCL20 recruits $CCR6^{+}$ Th17 cells. TL1A and IL-23 further activate Th17 cells to produce IL-17, which drives additional neutrophil-attracting chemokines and adhesion molecules, thereby promoting further neutrophil recruitment and epithelial barrier damage. Created in BioRender. Hang, S.(2026) https://BioRender.com/s711r2t.

Supplementary Table 1: Flow cytometry antibodies used in this study

Target	Clone	Fluoro-chrome	Vendor	Catalog #	Working dilution
CD354 / TREM1 (human)	TREM-26	APC	BioLegend	314909	1:200
CD45 (mouse)	30-F11	BV510	BioLegend	103138	1:400
CD11b (mouse)	M1/70	PE-Cy7	Invitrogen	46-0112-82	1:400
Ly6G (mouse)	1A8	FITC	BioLegend	127607	1:400
Ly6C (mouse)	AL-21	APC	BioLegend	128016	1:400
CD64 (mouse)	X54-5/7.1	BV605	BioLegend	139323	1:400
CD4 (mouse)	GK1.5	BV421	BD Biosciences	562891	1:400
TCRβ (mouse)	H57-597	PerCP-Cy5.5	BD Biosciences	561393	1:400
IL-17A (mouse, intracellular)	TC11-18H10.1	PE	BioLegend	506904	1:400

1. Kong, L. *et al.* Single-cell and spatial transcriptomics of stricturing Crohn's disease highlights a fibrosis-associated network. *Nat. Genet.* **57**, 1742–1753 (2025).